

Electronic Supplementary Material for:

**Multifunctional polyetheramine-epoxide gels and their prospective applications in
health and agriculture.**

*Heber E. Andrada¹, Bruno A. Fico¹, Felipe B. Alves¹, Julia M. Paulino¹, Natalia N. Silveira¹,
Raquel A. Dos Santos¹, Gabriel S. Montanha^{2,3}, Laura G. Nuevo², Hudson W. P. de Carvalho^{2,4},
Eduardo F. Molina^{1*}*

¹ *Universidade de Franca, Av. Dr. Armando Salles Oliveira 201, Franca, SP, 14404-600, Brazil*

² *Grupo de Estudo em Fertilizantes Especiais e Nutrição, Centro de Energia Nuclear na Agricultura,
Universidade de São Paulo, Av. Centerário 303, Piracicaba, SP, 13400-970, Brazil*

³ *Dipartimento di Biologia e Biotecnologie Charles Darwin, Sapienza Università degli Studi di Roma 'La
Sapienza', Via dei Sardi 70, Roma, RM, 00185, Italy.*

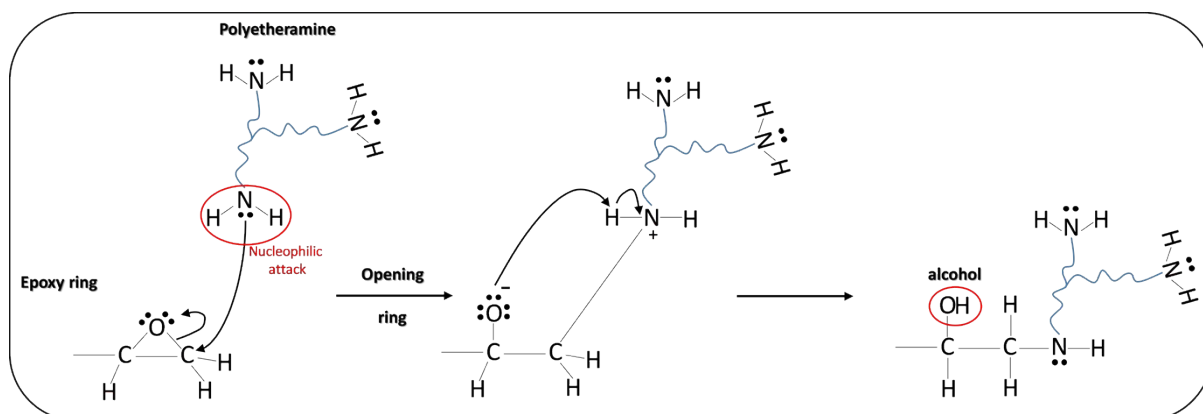
⁴ *Chair of Soil Science, Mohammed VI Polytechnic University, Lot 660, Ben Guerir 43150, Morocco.*

*Contact Author **e-mail:** eduardo.molina@unifran.br

Experimental

Materials: Diepoxy poly(ethylene glycol) (DPEG, $C_3H_5O_2-(C_2H_4O)_n-C_3H_5O$, average $M_w = 500 \text{ g mol}^{-1}$; CAS 26403-72-5), ciprofloxacin hydrochloride ($C_{17}H_{18}FN_3O_3$; CAS 86393-32-0), Iron-sodium ethylenediaminetetraacetate were purchased from Sigma-Aldrich. Jeffamine[®] poly(propylene oxide)-containing triamine T-5000 (polyetheramine PPO, $M_w = 5000 \text{ g mol}^{-1}$) was donated by Huntsman Chemical. All reagents were used as received. The cucumber seed (*Cucumis sativus*) were purchased from Isla Sementes Ltda (number 152732-001).

Synthesis of the polyetheramine-epoxide nanogels (PPO-DPEG): PPO-DPEG was synthesized by an aggregation polymerization process. [1] The monomers PPO and DPEG are both water soluble. Firstly, the DPEG monomer was dissolved in 10 mL of deionized water and left to stand for 60 min at 65 °C, under stirring. After, PPO polyetheramine was then added dropwise to the DPEG solution until complete dissolution. The PPO dropwise following by complete dissolution takes 20 s. The resulting solution was cooled to room temperature. The monomers concentration in water was 10 wt%. Nanogels were prepared using two different PPO-DPEG stoichiometric ratios: 1:1 (named NanoG1) and 1:3 (named NanoG2). For NanoG1, 0.9 g of PPO and 0.1 g of DPEG were used, while for NanoG2, 0.3 g of PPO and 0.1 g of DPEG were used. **Figure 1** (see manuscript) shows a schematic diagram of the nanogel preparation procedure. The chemistry of the amine-epoxide nanogels is based on nucleophilic addition which the amine attacks the electrophilic C of the C-O bond causing it to break, resulting in ring opening. Thus, the ring strain is relived and typically alcohols products are formed (see mechanism below)



Scheme S1: General mechanism for polyetheramine-epoxide for opening ring following by the alcohol formation as product of the reaction.

Characterization of the PPO-DPEG nanogels

Dynamic light scattering (DLS) and zeta potential (ζ): The hydrodynamic diameter (D_h), polydispersity index (PDI), and zeta potential (ζ) values of the nanogels were determined by DLS, using a ZSU3100 Zetasizer Lab Blue instrument (Malvern Panalytical) equipped with an OBIS solid state laser source ($\lambda = 633$ nm). The surface charge (in mV) of the nanogels was investigated by ζ measurements. DLS measurements using the individual monomers (PPO and DPEG) in solution with the same proportions used during the synthesis of NanoG1 and NanoG2 were performed. The results demonstrated very different results for the particles formed (hydrodynamic size) obtained after amine-epoxide reactions (see Figure S1).

Thermogravimetric analysis (TGA): TGA measurements of the nanogels were performed using an SDT Q600 system (TA Instruments Inc., USA). An approximately 20 mg portion of the lyophilized nanogel (NanoG1 and NanoG2) was placed in a standard aluminum pan and heated from 25 to 700 °C, at a rate of 10 °C/min, under a 100 mL min⁻¹ flow of nitrogen.

Transmission electron microscopy (TEM): The morphologies of the PPO-DPEG nanogels were characterized by TEM, using a JEM 100CXII instrument (JEOL) operating at 100 kV. For the analysis, the nanogel was transferred to a copper grid, followed by drying.

Ultra-small angle X-ray scattering (USAXS): USAXS was performed at the CATERETÊ beamline (Brazilian Center for Research in Energy and Materials (CNPEM)) at a photon energy of 10 keV (1% bandwidth). The scattered photons were detected using a PiMega540D detector at a sample-detector distance of 15 m, covering a q range of 0.005 - 0.58 nm⁻¹. The nanogel sample (10 wt%) was filled into 1.5 mm diameter quartz capillaries and heated to 65°C.

Cell culture and cytotoxicity of nanogels by XTT colorimetric assay: The GM07492A cell line (normal human lung fibroblasts), obtained from Coriell Cell Repositories (USA), was cultivated in DMEM+HAM F10 (1:1, v/v) (Sigma, St Louis, USA) supplemented with 10% fetal calf serum (Sigma, St Louis, USA) and 1% penicillin/streptomycin stabilized solution (Sigma, St Louis, USA). The cells were cultured in T25 flasks (TPP, Switzerland) at 37 °C, in the presence of 5% CO₂, and were used between the third and eighth passage. Cytotoxicity was determined using the XTT assay.^[2,3] For this, 3x10⁴ cells/well were seeded in a 96-well plate. After 24 h, the cell culture was treated with different concentrations of NanoG1 and NanoG2, followed by incubation for an additional 72 h. The negative control received no treatment, the positive control received a final concentration of 10% DMSO (Sigma, St Louis, USA), and the

solvent control received 10% of Milli-Q water. The plate was washed twice in phosphate buffered saline (PBS, 1X) and incubated for 4 h, at 37 °C, using DMEM without phenol red and supplemented with the reagents of the Cell Proliferation Kit (Roche), as recommended by the manufacturer. Total absorbance was measured at 492 and 690 nm, using a microplate reader (ASYS, Eugendorf, Salzburg, Austria). The total absorbance values were considered directly proportional to the number of viable cells as a percentage of the negative control (100% cell viability). Statistical calculation of the IC₅₀ value was performed to determine the sample concentration that caused 50% inhibition of cell viability. All the statistical tests and the IC₅₀ calculations employed GraphPad Prism v. 5.0 software. Comparative analysis among the experimental groups employed analysis of variance (ANOVA), followed by the Tukey test when significant differences among treatments were found. The significance was set at $p < 0.05$ and the results were reported as means and standard deviations (SD) of three independent experimental samples analyzed in triplicates.

***In situ* UV-Vis drug release assays:** Loading of ciprofloxacin into the nanogels was achieved by a simple incubation method. Drug-loaded nanogels were prepared by dissolving ciprofloxacin at 1 wt% in the DPEG monomer solution. The same procedure described above for synthesis of the PPO-DPEG nanogel was then followed, adding PPO dropwise, to obtain loaded NanoG1 and loaded NanoG2. To investigate the amount of ciprofloxacin release, the obtained loaded-nanogels were lyophilized and placed into dialysis tube (MWCO 14000) and then dispersed into 10 mL of deionized water. After this suspension was dialyzed against 100 mL of deionized water, at 37 °C, under constant agitation. The system was covered with aluminum foil to prevent degradation of the drug by light irradiation. The *in situ* analysis employed a Cary 60 UV-Vis spectrophotometer (Agilent) coupled to a fiber optic immersion probe. The instrument was controlled using CaryWin Scan software, with UV-Vis spectra (absorbance according to wavelength) recorded at predetermined times. The results were reported as the mean for three independent experimental samples, each of which was analyzed in triplicate. Aqueous standard solutions of the drug at different concentrations were used to construct a calibration curve (**Figure S2**) for quantitative determination of ciprofloxacin ($\lambda_{\text{max}} = 280$ nm) in the solution during the release assay. All measurements were performed in triplicate. Ciprofloxacin entrapment efficiency (CEE) was detailed in Support Information (see Equation 1).

Seed treatment: Cucumber seeds (*Cucumis sativus*) were surface-sterilized in sequential washes for 15 min in 2% sodium hypochlorite, and three times in deionized water. The nanogel

solution was applied to seeds to study the evolution on the shoot/root height (seed germination) of cucumber plant. For this, 20 seeds were added into a flask containing 10 mL of the nanogel solution and then the flask was left to 24h in the dark at room temperature before germination on Petri dishes. Another batch using water (without nanogel) was prepared as a control. The coating seeds (treatment with nanogel or water) were placed on the filter paper in the Petri dishes with five seeds per dish, sealed with Parafilm, inserted into a plastic bag to prevent water loss. Four replicates of the assays were conducted per treatment.^[4] The seeds assays (treatment) with iron (Fe) were performed using the same procedure cited above in which Iron(III)-sodium ethylenediaminetetraacetate solution (at concentration of 100 mg L⁻¹) was used as control and another batch employing embedded NanoG1 containing 100 mg L⁻¹ of the same Fe solution was used for comparison. The embedded NanoG1 was prepared via solubilization of 10 mg portion of the lyophilized NanoG1 in 10 mL of the Fe solution (100 mg L⁻¹). Iron(III)-sodium ethylenediaminetetraacetate is commonly used in agricultural applications.

Assessment of Fe distribution in soaked seeds by microprobe X-ray fluorescence spectroscopy (μ -XRF): Mature *Cucumis sativus* seeds soaked either with the positive control (Fe-solution) or NanoG1-Fe, as previously described, were manually cross-sectioned at the median region using a razor blade and preserving the embryo region. Then, the samples were fixed within two layers of a 6- μ m thick polypropylene film (VHG, FPPP25-R3), mounted in an X-ray sample cup (Chemplex no.1530) and immediately loaded into the μ -XRF spectrometer (Orbis PC, Edax, USA). The Fe distribution was evaluated through a 64-point linescanning across the embryo or cotyledonary tissues, as shown in **Figure S8**, as well as by 800-pixel maps, through a 30 μ m polycapillary-focused X-ray beam operating at 22.5 W and 250- μ m thick Al primary filter selected. For the linescans, each point was irradiated by 15 s, whereas 1 s pixel⁻¹ dwell-time was employed for the maps. The analyses were carried out under atmosphere conditions and the spectra were recorded by a 30 mm² silicon-drift detector (SDD) with a dead-time smaller than 2%. The XRF linescans were conducted using 3 independent biological replicates, whereas the maps were recorded in one. In both analyses, only the Fe intensities above the instrumental limit of detection (LOD), calculated according to the equation S1 below, were considered valid :

Equation S1.
$$LOD = 6 \cdot \sqrt{2 \cdot \left(\frac{BG}{t}\right)}$$

Where : BG (cps) is the elemental background counting rate* and t (s) is the acquisition time. * for the XRF maps, the average of 10 random background measurements were considered.

Finally, the Fe intensities recorded across each sampled tissues, *i.e.*, seed coat, embryo, or cotyledon were obtained from the linescan analyses. For each tissue, the values obtained at both control and treated seeds were subjected to Shapiro-Wilk normality test at a 95% confidence interval ($p > 0.05$) and compared through the Kolmogorov–Smirnov t-test. All analyses were conducted using Prism software (version 9.2.0, GraphPad, USA).

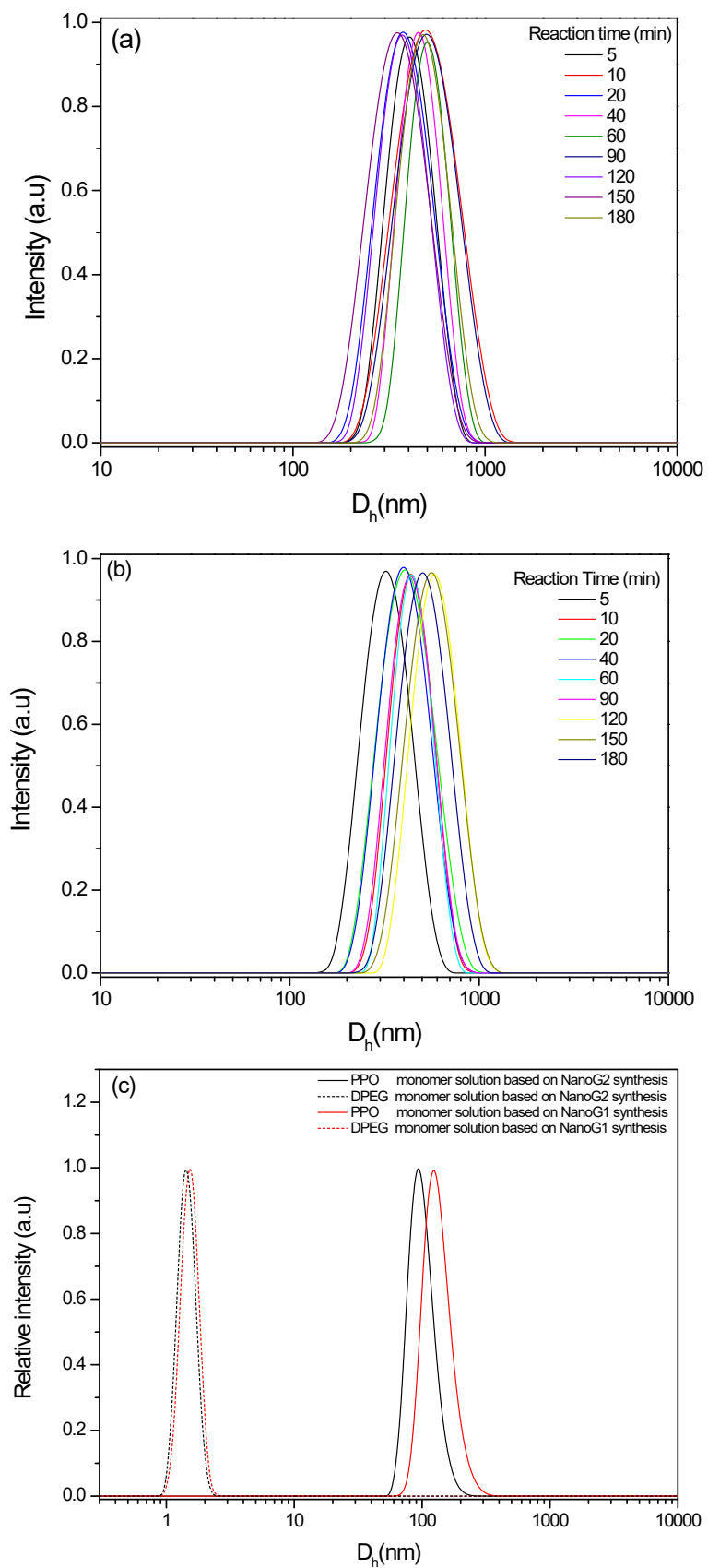


Figure S1. Evolution of the hydrodynamic diameter (D_h) of the nanogels as a function of reaction time for (a) NanoG1 and (b) NanoG2; (c) DLS measurements using the individual monomers (PPO and DPEG) in solution with the same proportions used during the synthesis of NanoG1 and NanoG2.

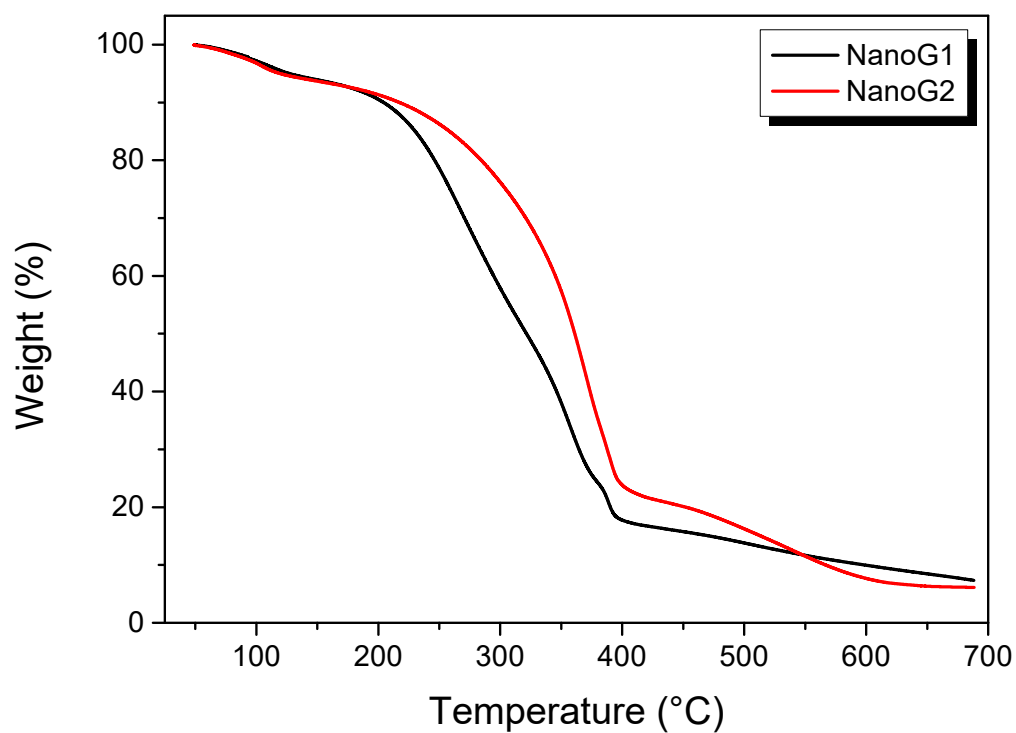


Figure S2. Thermogravimetric analysis (TGA) curves for the decomposition of NanoG1 (black line) and NanoG2 (red line).

USAXS Data reduction and azimuthal integration were carried out using PyFAI.^[5] Model dependent analysis, Guinier fitting, was performed using SasView.^[6]

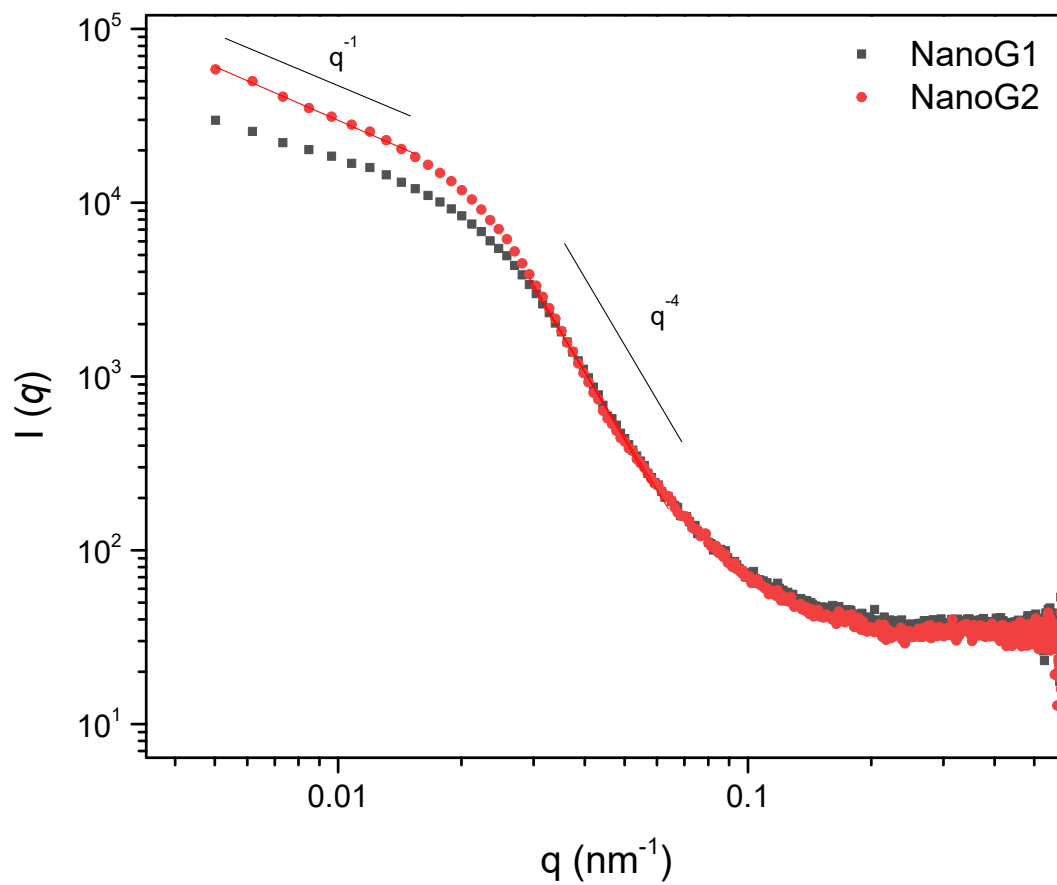


Figure S3. USAXS pattern for nanoG1 (black squares) and NanoG2 (red circles).

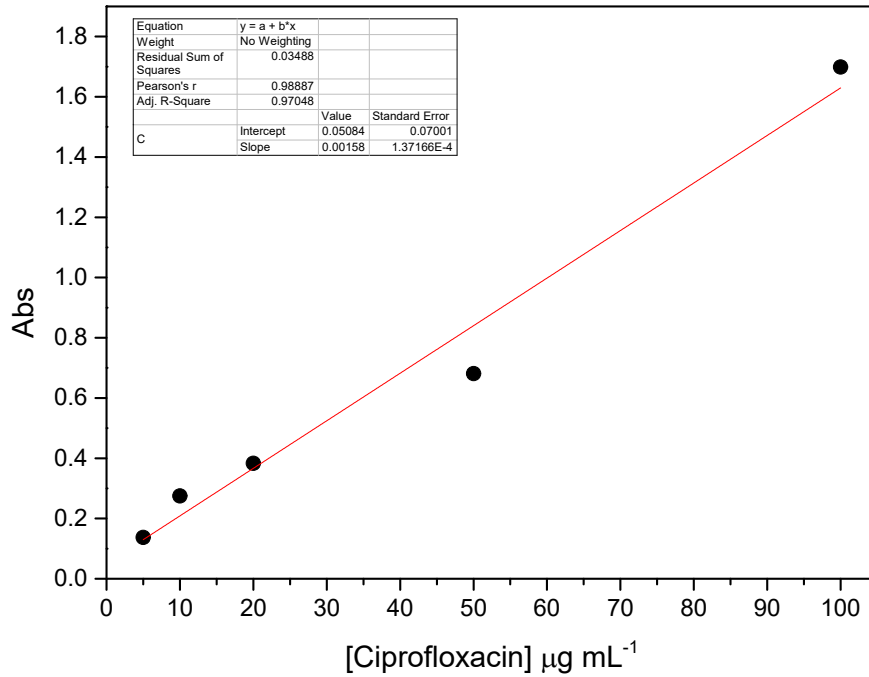


Figure S4. Calibration curve of ciprofloxacin obtained by UV-vis spectroscopy using maximum absorbance of the drug molecule $\lambda_{\text{max}} = 280$ nm.

Ciprofloxacin drug entrapment efficiency were defined as follow:

$$\text{(CEE) Ciprofloxacin entrapment efficiency (\%)} = \frac{W_{\text{cipro}}}{W_{\text{Lcipro}}} \times 100 \quad (\text{Eq 1})$$

where W_{cipro} was the weight of ciprofloxacin in the lyophilized nanogel, which was calculated as the total released weight of ciprofloxacin from nanogel, and W_{Lcipro} was the loaded weight of ciprofloxacin. For NanoG1 and NanoG2 the CEE were determined at 89.7% and 90.5 %.

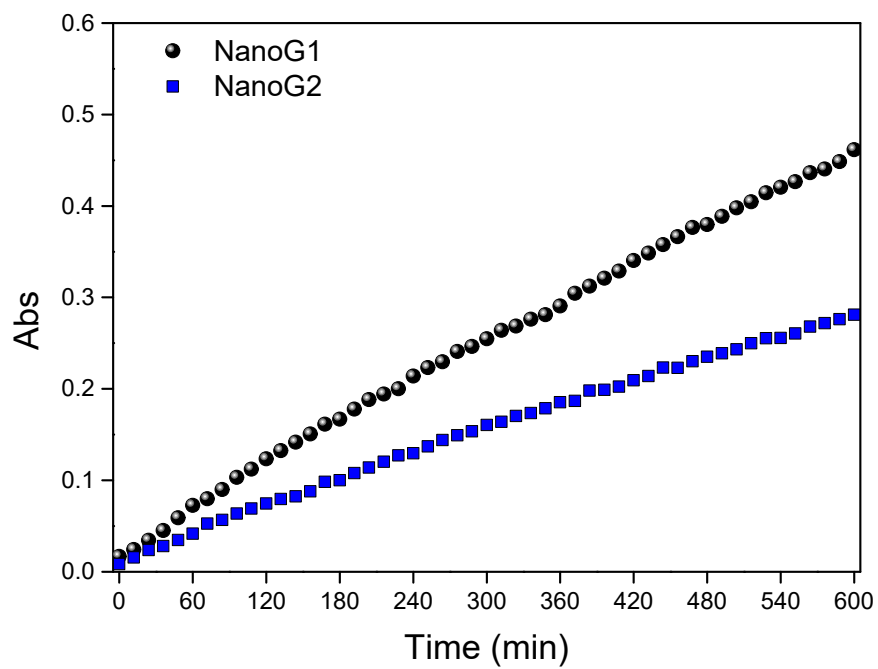


Figure S5. Time evolution of ciprofloxacin absorbance at $\lambda_{\text{max}} = 280$ from NanoG1 (black circles) and NanoG2 (blue squares).

Kinect release model:

Korsmeyer–Peppas [7] kinect model was applied to the drug release curves. Korsmeyer–Peppas model assumes a power law dependence to describe diffusion-controlled (Fickian) and swelling-controlled (Case II transport) mechanisms:

$$\frac{M_t}{M_\infty} = k t^n \quad \text{or} \quad \log \frac{M_t}{M_\infty} = \log k + n \log t$$

where M_t is the drug mass released at time t , M_∞ is the drug mass at $t = 0$, M_t/M_∞ is a fraction of the drug released at time t , k is the released rate constant and n is the released exponent which gives information regarding the drug transport mechanism. $n = 1$ characterized Case II transport indicate zero-order drug release, values of $n = 0.5$ indicate Fickian diffusion and n values between 0.50 and 0.90 can be regarded as an indication of the existence of both phenomena (anomalous transport).

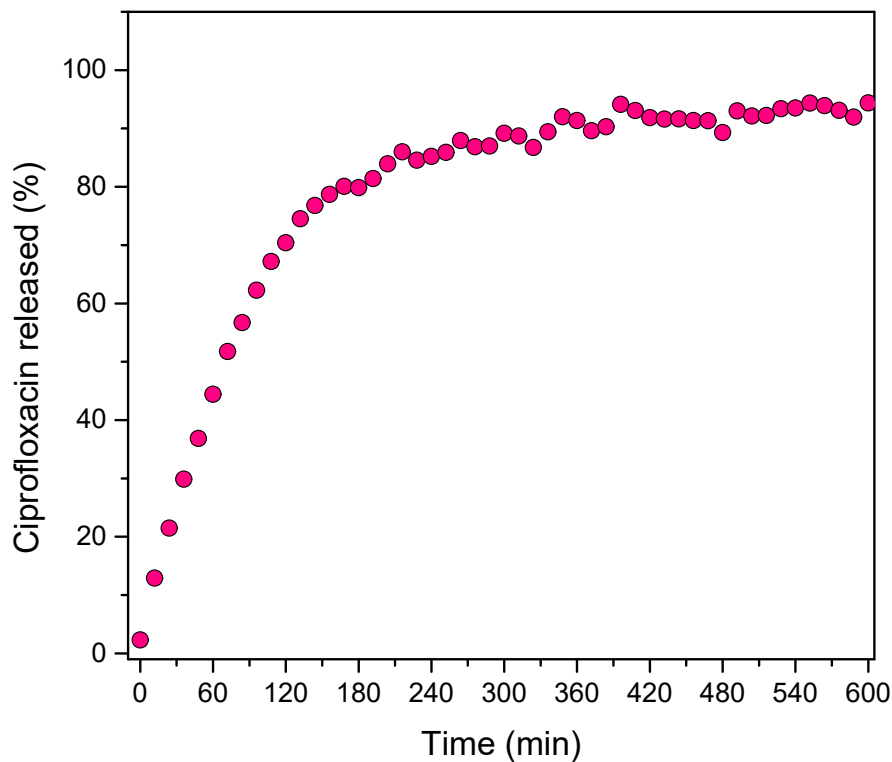


Figure S6. Release profile of free ciprofloxacin as a function of time. The same condition such as dialysis bag, ciprofloxacin concentration, and water volume was use for comparison with release assays from NanoG1 and NanoG2.

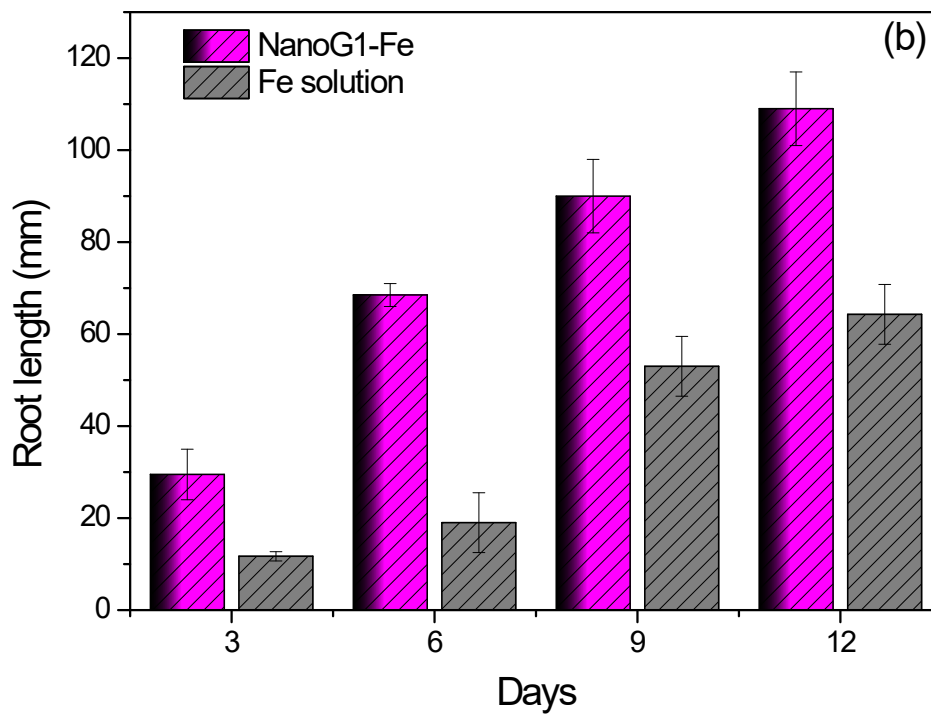
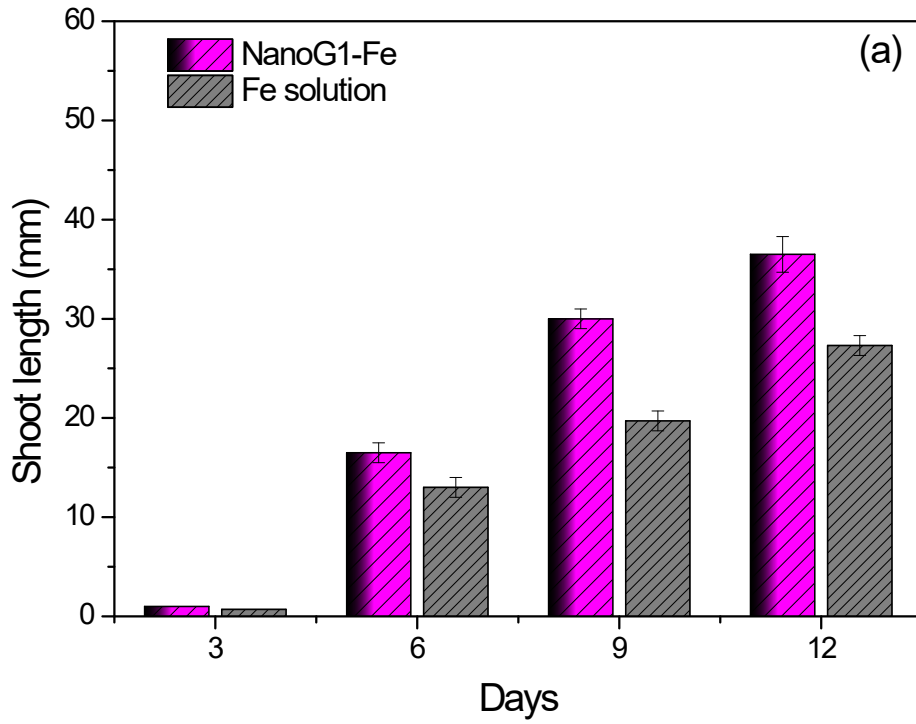


Figure S7. Initial seedling growth during 12 days after sowing: (a) shoot length (mm); (b) root length (mm) using NanoG1 and a Fe solution at the concentration of 100 mg L^{-1} . All the results represent the average of 4 Petri plates, containing a total of 5 seeds per plate.

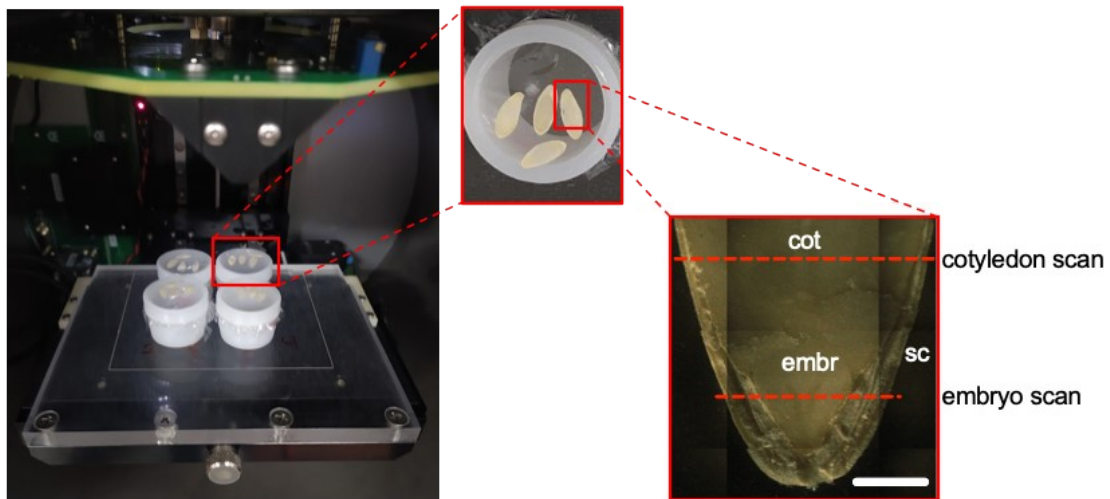


Figure S8. Details of the samples and experimental setup employed for μ -XRF assessment of Fe distribution in cucumber seeds. Scale: 1 mm.

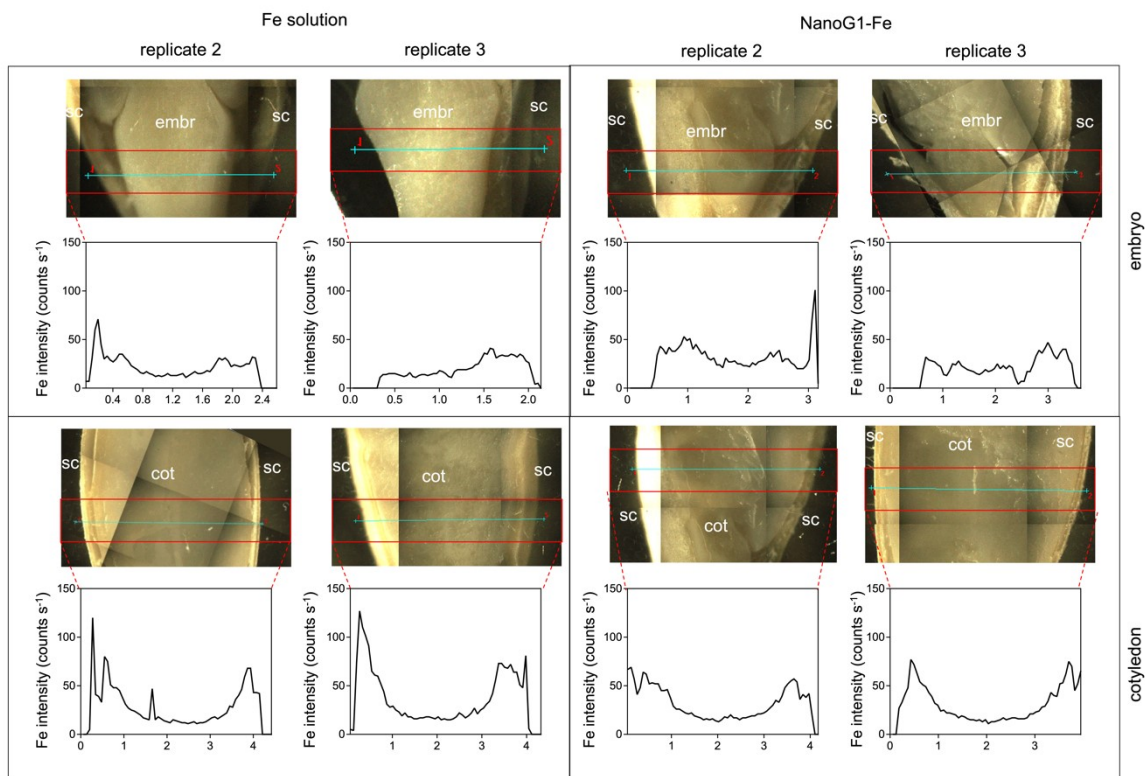


Figure S9. Microprobe XRF scanning of Fe distribution in cucumber seeds cross-sections primed with either the positive control (Fe solution) or NanoG1-Fe solutions. Data from biological replicates. sc: seed coat; embr: embryo; cot: cotyledon.

Table S1. hydrodynamic diameter (D_h) and polydispersity (PDI) values for NanoG1 and NanoG2 nanogels as a function of time reaction.

Reaction Time (min)	NanoG1		NanoG2	
	D_h (nm)	PDI	D_h (nm)	PDI
5	432 ±20	0.14	334 ±16	0.10
20	408 ±23	0.14	430 ±21	0.14
40	403 ±23	0.20	416 ±20	0.14
60	405 ±26	0.20	454 ±22	0.18
90	438 ±26	0.10	446 ±22	0.15
120	397 ±20	0.14	600 ±21	0.15
150	438 ±28	0.24	523 ±26	0.15
180	447 ±25	0.10	462 ±23	0.20

References:

- [1] S. Tang, Z. Shi, Y. Cao, W. He, *J. Mater. Chem. B* **2013**, 1 (11), 1628–1634.
- [2] D.A. Scudiero, R.H. Shoemaker, K.D. Paull, A. Monks, S. Tierney, T.H. Nofziger, *Cancer Res.* **1988**, 48 (17), 4827–4833.
- [3] R.R. Neubig, M. Spedding, T. Kenakin, A. Christopoulos. *Pharmacol. Rev.* **2003**, 55 (4), 597–606.
- [4] A. E.S. Pereira, H.C. Oliveira, L.F. Fraceto, *Scientific Reports* 2019, 9 (1).
- [5] PyFAI, a versatile library for azimuthal regrouping J. Kieffer & D. Karkoulis *J. Phys.: Conf. Ser.* 425 202012.
- [6] M. Doucet, J.H. Cho, G. Alina, J. Bakker, W. Bouwman, P. Butler, K. Campbell, M. Gonzales, R. Heenan, A. Jackson, P. Juhas, S. King, P. Kienzle, J. Krzywon, A. Markvardsen, T. Nielsen, L. O’Driscoll, W. Potrzebowski, L.R. Ferraz, T. Richter, P. Rozycko, T. Snow, A. Washington, *SasView Version 5.0.5*, **2017**, Available online at: <http://www.sasview.org>.
- [7] R. W. Kormsmeier, R. Gurny, E. Doelker, P. Buri, N.A. Peppas, *Int. J. Pharm.* **1983**, 15, 25–35.